https://doi.org/10.1016/j.scitotenv.2019.134306

Exploring how fire spread mode shapes the composition of pyrogenic carbon from burning forest litter fuels in a combustion wind tunnel

N. C. Surawski[1, *, †], L. M. Macdonald[2], J. A. Baldock[2], A. L. Sullivan[1], S. H. Roxburgh[1], P. J. Polglase[1,3]

[1] CSIRO Land and Water, GPO Box 1700, Canberra, Australian Capital Territory 2601, Australia

[†] Current address: School of Civil and Environmental Engineering, University of Technology Sydney, Ultimo, New South Wales 2007, Australia

[2] CSIRO Agriculture and Food, Locked Bag 2, Glen Osmond, South Australia 5064, Australia

[3] School of Ecosystem and Forest Sciences, The University of Melbourne, Parkville, Victoria 3010, Australia

* Corresponding author:

N. C. Surawski, email address: Nicholas.Surawski@uts.edu.au

Abstract

In this study, solid state ^{13}C nuclear magnetic resonance (NMR) spectroscopy was used to explore the carbon-containing functional groups present in pyrogenic carbon (PyC) produced during different fire spread modes to forest litter fuels from a dry sclerophyll eucalypt forest burnt in a combustion wind tunnel. A replicated experimental study was performed using three different fire spread modes: heading fires (i.e. fires which spread with the wind), flanking fires (i.e. fires which spread perpendicular to the wind) and backing fires (i.e. fires which spread against the wind). In addition to ^{13}C NMR measurements of PyC, detailed fire behaviour measurements were recorded during experiments. Experiments showed that heading fires produced significantly more aryl carbon in ash samples than flanking fires. All other experimental comparisons for burnt fuel samples involving different fire spread modes were statistically insignificant. Principal component analysis (PCA) was used to explore the relationship between ^{13}C NMR functional groups and fire behaviour observations. Results from PCA indicate that maximising the residence time of high temperature combustion and the combustion factor (i.e. the fraction of pre-fire biomass consumed by fire) could be a method for increasing the amount of aryl carbon in PyC. Maximising the amount of aryl carbon could be beneficial for the overall PyC balance from fire, since more recalcitrant carbon (e.g. carbon with a higher aryl carbon content) that is not emitted to the atmosphere has been shown to have longer residence times in environmental media such as soils or sediments.

1. Introduction

Wildland fire plays a significant role in the biogeochemical cycling of carbon including influences on global climate through its release of greenhouse emissions species and black carbon (Bond et al., 2013; Andreae, 2019). Recent estimates from the fourth version of the Global Fire Emissions Database suggest that an average of 2.2×10^{15} grams of carbon were emitted from wildland fire annually between 1997 and 2016 (van der Werf et al., 2017). Based on data from Le Quere et al. (2018), wildland fire therefore emits approximately 22 % of annual anthropogenic emissions from fossil fuel combustion and industry over the period 2007-2016. Although wildland fires are sometimes considered to be carbon neutral disturbances due to post-fire carbon sequestration from regrowth of vegetation (Bowman et al., 2009), this outcome is not achieved in deforestation fires where vegetation does not grow back (van der Werf et al., 2010) or when old carbon stocks are burnt such as in peatland fires (Page et al., 2002). More comprehensive assessments of carbon balance also consider the production of pyrogenic carbon (PyC) that is thermochemically altered (pyrolysed) carbon formed from the incomplete combustion of organic matter during biomass burning or fossil fuel consumption (Bird et al., 2015). The current work focusses on the carbon-containing functional groups present in PyC that are produced by biomass burning, are not emitted to the atmosphere and are potentially a source of long term carbon sequestration when stored in soils or sediments (Forbes et al., 2006; Santin et al., 2015; Santin et al., 2016). The chemical composition of PyC is broad and sits on a continuum spanning from biomass that has been slightly charred to that of condensed phase aromatic carbon (Masiello, 2004; Krishnaraj et al., 2016). Recent insights on how the longevity (or recalcitrance) of PyC is affected by the pyrolysis process and its relationship with PyCs physico-chemical composition is provided by Santin et al. (2017).

Prescribed fire is a land management operation that is widely undertaken worldwide that involves the intentional application of fire to the landscape (Penman et al., 2011) to achieve specific management objectives such as hazard reduction, site preparation or ecological regeneration. Prescribed burning is often undertaken to mitigate against the unwanted consequences of wildfire (Jenkins et al., 2016) and has the potential to alter the stocks of PyC in soils (Jenkins et al., 2014). From a carbon management perspective, prescribed burning potentially offers the opportunity to manipulate greenhouse gas emissions and PyC production properties in a controlled manner which can be contrasted with the wildfire scenario where such control is not possible.

Out of the fire management techniques explored to reduce the carbon impact from prescribed fire, one that has not received any significant research attention is the intentional application of different fire spread modes (FSMs). Fire spread is described using three predominant modes (Figure 1): heading, in which the fire spreads with and parallel to the direction of the prevailing wind; flanking, in which the fire spreads perpendicular to the prevailing wind direction; and backing, in which the fire spreads against the wind. A fire starting from a point will develop a fire perimeter in which all three fire spread modes are present around the perimeter. Different FSMs, being driven by the relative direction of fire spread with respect to the direction of the prevailing wind, have distinct differences in fire behaviour, particularly combustion rate, rate of spread, fireline intensity, heat release rate, and flame height (Surawski et al., 2015).

Initial savannah fire studies conducted by biogeochemists and atmospheric scientists in Africa investigated the relationship between FSM and carbon dynamics with results hinting at the possibility that fire behaviour may influence the amount or type of carbon either released

to the atmosphere or remaining on the ground after fire (Kuhlbusch et al., 1996; Lacaux et al., 1996; Wooster et al., 2011). Figure 1 shows that different FSMs of an intentionally lit fire can be achieved by altering the ignition position in a fuel bed relative to the direction of the prevailing wind. Modulating the applied fire spread mode by changing the ignition pattern results in the desired direction of fire spread being achieved, as is done (for example) for prescribed burning in Victoria, Australia (Tolhurst and Cheney, 1999) and Florida, United States (Carvalho et al., 2011). Further investigations undertaken by forestry professionals in the United States (National Wildfire Coordinating Group Fire Use Working Team, 2001), which were advanced by Keene et al. (2006) and Surawski et al. (2015) have provided empirical evidence that the preferential application of flanking and backing fires over heading fires has the potential to positively modulate the greenhouse gas emissions and PyC formation patterns (both in terms of the absolute and relative amount of PyC produced) from a propagating fire. The application of different FSMs is potentially of interest to the management of prescribed burning operations from a carbon perspective since a field study conducted in the south-eastern United States indicated that charcoal production could be doubled ($p < 0.001$) by the preferential application of backing fires over heading fires (Carvalho et al., 2011). In addition, theoretical insights from the thermokinetics of biomass combustion suggest that FSM has the potential to modulate not only the type and amount of carbon released to the atmosphere, but also the type and amount of PyC (e.g. different carbon-containing functional groups) that remains on the ground after fire (Sullivan, 2007; Sullivan and Ball, 2012).

In this study, we employ solid state ^{13}C nuclear magnetic resonance (^{13}C NMR) spectroscopy (Wilson, 1987; Simpson et al., 2011) as an analytical technique to explore the change in carbon-containing functional groups associated with the production of PyC from different

FSMs. Based on the findings of Sullivan (2007) and Sullivan and Ball (2012), the working hypothesis for the present investigation is that the application of different FSMs will alter the type of functional groups present in PyC as determined by ^{13}C NMR spectroscopy. In particular, we are interested in enhancements of aryl and O-aryl carbon concentrations from the application of different FSMs since these types of carbon can potentially be sequestered in soils and sediments longer than more labile carbon types such as alkyl and O-aryl carbon (Hilscher and Knicker, 2011). Investigating this hypothesis extends the work of Surawski et al. (2015) who showed that flanking and backing fires produce more PyC than heading fires. In the previous study (Surawski et al., 2015), the relationship between fire behaviour and greenhouse gas emissions was explored, whereas this work targets the relationship between fire behaviour and the subsequent production of PyC that is not emitted to the atmosphere and remains on the ground after fire.

2. Methodology

While a brief overview is provided here, a detailed description of the experimental design that underpins this combustion wind tunnel study can be found in Surawski et al. (2015). Surawski et al. (2015) also provide a more detailed description of the fuel collection and handling protocols, the design features of the CSIRO Pyrotron combustion wind tunnel facility, as well as the design of the experiment from a fire behaviour perspective. In addition, it should be noted that as our study focused on outcomes from free-burning vegetation fires, our experimental fires were allowed to combust completely (i.e. involving flaming, smouldering and glowing combustion) and thus were not restricted to pyrolysis in isolation.

2.1 Fuel collection and handling

Forest litter fuel for the experimental fires was collected from Kowen Forest (situated in the north-east of the Australian Capital Territory, Australia; coordinates 35.31982 °S 149.26461

°E) in a stand dominated by *Eucalyptus macrorhyncha* (F. Muell.) and *E. rossii* (R. T. Bak. & H. G. Sm). An attempt was made during the fuel collection to only include fine fuels (< 6 mm in diameter) which are those fuels consumed in an active fire front (Sullivan, 2017), consisting of leaves, bark and twigs for this forest type. Fuels were sieved after collection in the field to remove coarse fuel elements (≥ 6 mm in diameter) and decomposed fuel from the soil fermentation layer that would affect the ability of experimental fires to propagate.

A dry fine fuel load of 1.1 kg m^{-2} was used in all experiments which is based on the typical fine fuel loads measured from a major Australian wildfire in dry sclerophyll forest by Cruz et al. (2012). Measuring the fine fuel moisture content with a Wiltronics fine fuel moisture meter (Chatto and Tolhurst, 1997) ensured that the correct dry fuel load was achieved for each fire. Fine fuels were dried in an oven at 50 °C for 24 hours to achieve a fine fuel moisture level (Table 1) typical of that achieved during Australian wildfires (McArthur, 1967; Cruz et al., 2012; Sullivan and Matthews, 2013).

2.2 Combustion wind tunnel details

Experiments were performed using the Commonwealth Scientific and Industrial Research Organisation (CSIRO) Pyrotron (Sullivan et al., 2013) which is a 25.6 m long combustion wind tunnel that is designed to investigate the behaviour (Mulvaney et al., 2016; Sullivan et al., 2018), carbon emissions (Surawski et al., 2015) and suppression characteristics (Plucinski et al., 2017) of free-spreading laboratory-scale fires. Upstream of the working section, a 1.372 m diameter centrifugal fan (model 54LSW; Fans and Blowers Australia Pty Ltd) provides wind that is directed through a series of perforated screens and flow straighteners to reduce the turbulence intensity of the air stream below 0.6 % (Sullivan et al., 2013). Downstream of the fan and flow straighteners, experimental fires took place in the working

section which is 1.5 m wide and 4.8 m long. An array of K-type thermocouples was placed on the Pyrotron floor that enabled temperature measurements to be made near the base of (i.e. 2-3 cm above) the passing flames (Figure 2).

2.3 Fire behaviour experimental design

The design of this experiment was motivated by previous research studies (Kuhlbusch et al., 1996; Lacaux et al., 1996; National Wildfire Coordinating Group Fire Use Working Team, 2001; Keene et al., 2006; Wooster et al., 2011; Surawski et al., 2015) indicating that fire behaviour and carbon emissions are potentially influenced by the applied FSM. In this study, the three distinct modes of fire spread with respect to the prevailing wind direction, heading, flanking and backing, were investigated (Figure 2). Experimental fires were not considered complete until all flaming and smouldering combustion had ceased. Although fire behaviour and greenhouse gas emissions data were collected from six fires for each FSM (i.e. 18 experimental fires in total; Surawski et al., 2015), PyC samples were only collected using three replicates (i.e. nine experimental fires in total). In addition, the fire behaviour data reported in this study involves the same fires for which PyC data were collected.

2.4 Post-fire sampling

After the completion of experimental fires, PyC (i.e. fuel that was thermochemically altered due to exposure to flame but not emitted to the atmosphere) was allowed to cool down before performing post-fire sampling (see Figure 3 for a typical post-fire fuel bed). A circular metal ring with a cross-sectional area of 0.05 m^2 was used to isolate an area of the burnt fuel bed for subsequent ^{13}C NMR analysis. The metal ring was positioned along the centreline and within the last 0.5 m of the burnt fuel bed with respect to the direction of applied fire spread. The isolated patch within the burnt fuel bed was swept up with a firm bristled brush and placed into aluminium trays. After its collection, PyC was sorted into four fuel fractions, either burnt

leaves, burnt twigs, burnt bark or ash, and then weighed. From these measurements, the mass of PyC formed could be partitioned between burnt leaves, burnt twigs, burnt bark and ash (see Figure 4) and expressed as a percentage of the total mass of fuel burnt. We define ash as the visually white and grey material remaining after combustion. While ash is often considered to contain inorganic species only (Raison et al., 1985), we did not remove the very finely sized carbon particles within it. Therefore our ash samples still contain some carbon and qualify as PyC. Our definition for determining post-fire PyC follows that of Bird et al. (2015) which involves "thermochemically altered" fuel, which is consistent with the notion of "burnt" fuel discussed in Surawski et al. (2016). A visually representative fraction from each of the four fuel fractions was placed into sealed plastic vials prior to ^{13}C NMR analysis. Samples were transported to the laboratory and were stored at room temperature before analysis.

2.5 ^{13}C NMR analysis protocols

Overall, the ^{13}C NMR analysis protocols closely follow that of Baldock et al. (2013) which we overview here. Burnt and unburnt fuel samples were fine ground prior to solid state ^{13}C NMR spectroscopy to determine carbon chemistry. Weighed samples, of approximately100–600 mg, were packed into zirconia rotors with a 7-mm-diameter and Kel-F® end caps before being spun at 5 kHz. When samples did not fill the rotor completely, Kel-F inserts were used to fill any gaps and to place the sample in the middle of the rotor. A 200 Avance spectrometer (Bruker Corporation, Billerica, MA, USA) was used to acquire all ^{13}C NMR spectra. The spectrometer was equipped with a 4.7 T wide-bore superconducting magnet that operated at a resonance frequency of 50.33 MHz. Calibration of chemical shift values were performed using the methyl resonance of hexamethylbenzene at 17.36 ppm. In addition, a Lorentzian line broadening of 50 Hz was applied to all spectra. All spectral processing was completed with the Bruker TopSpin 3 software using the spectral region assignments for different

carbon-containing functional groups as presented in Table 2. All ^{13}C NMR analysis was performed using three replicates for each experimental treatment.

2.6 Statistical Analysis Methods

One-way analysis of variance was performed for each burnt fuel component to test whether ^{13}C NMR spectral composition depended on FSM. Tukey honest significant difference tests were used to assess the statistical significance of pairwise comparisons. Linear model assumptions were tested using the gvlma package in R (Pena and Slate, 2006; Pena and Slate, 2019). All analyses were performed in R version 3.4.0 (The R Foundation for Statistical Computing, 2017) with a 5 % level for statistical significance.

Principal component analysis (PCA; Wehrens, 2011) was performed to explore the relationship between samples based on the ^{13}C NMR functional groups present in fuel samples burnt with different FSMs as well as their relationship with recorded fire behaviour variables. PCA was performed in R using the FactoMineR package (Husson et al., 2018). All data were centred and standardised with unit variance before analysis which led to computations being performed with the correlation matrix. The factoextra package was used to visualise results (Kassambara and Mundt, 2017), with PCA biplots being used to show both scores and loadings from the analysis.

A few features inherent to the PCA biplot are worth noting. An attractive feature of the PCA biplot is its ability to capture information from the scores and loadings matrices in the one plot (Zuur et al., 2007). Since PCA involves projecting a higher dimensional space to one of lower dimensionality, observations are mapped and stored in a new co-ordinate space in the scores matrix. In contrast, the loadings matrix captures the contribution of the original

variable to a particular principal component (PC). In the PCA biplot, correlated variables (or observations) lie roughly parallel with each other (± 45 °), anti-correlated variables (or observations) lie roughly opposite one another (135-225 °) and un-correlated variables (or observations) are roughly orthogonal (45-135 °). Further, the length of an arrow indicates the degree of variability of a variable, with longer arrows indicating more variable data. Finally, observations that are found further from the origin in the PCA biplot indicate that the variable is strongly associated with that particular PC.

3 Results

A summary of the key fire behaviour variables relevant for this experiment is provided in Table 1. Compared to flanking and backing fires, heading fires exhibit a reduced duration of flaming combustion, a longer duration of smouldering combustion, a much higher rate of spread and Byram fireline intensity (Byram, 1959), and a higher $\Delta CO/\Delta CO_2$ emissions ratio. In contrast, temperature measurements made by the thermocouples are fairly similar between all three FSMs.

A graphical summary of the integrated ^{13}C NMR spectra for unburnt fuel samples is presented in Figure 5. For unburnt fuels, ten statistically significant differences were found for multiple comparisons involving carbon-containing functional groups for different vegetation components (Supplementary Tables 1 and 7). In terms of alkyl and aryl carbon, leaves had the highest concentrations followed by twigs and then bark, whereas for O-alkyl and di-O-alkyl carbon, bark had the highest concentrations followed by twigs and then leaves.

Figure 6 presents the percentage change in ^{13}C NMR composition associated with the application of a particular FSM to each vegetation component (i.e. leaves, twigs and bark) after burning. The largest changes in ^{13}C NMR composition from our fires were for reductions (i.e. combustion) of O-alkyl carbon, as well as enrichments (i.e. increases) in aryl carbon. Decreases in O-alkyl carbon concentrations ranged from 31% for heading and backing fires to 9% for flanking fires. Enrichments in aryl carbon ranged from 7% for flanking fires up to 28% for heading fires. Additionally, ash samples (Figure 7) are particularly enriched with aryl carbon, where approximately 36% of total carbon in ash is aryl carbon. For flanking and backing fires the percentage of total carbon in ash that is aryl carbon is approximately 26% and 31%, respectively.

Following on from Figure 6, the only statistically significant result for burnt fuels was an increase in aryl carbon for ash from heading fires compared to ash from flanking fires ($p = 0.0156$; Figure 7; Supplementary Table 11). No other burnt fuels yielded statistically significant differences in terms of the carbon-containing functional groups quantified. This includes also the production of PyC (Figure 4) whereby flanking and backing fires produce more PyC than heading fires; however, the difference is not statistically significant ($p = 0.176$; Supplementary Table 12). In addition Supplementary Tables 7, 8, 9 and 10 show results from statistical testing for unburnt fuels, as well as burnt leaves, burnt twigs and burnt bark.

While only one statistically significant result was found above, PCA sheds some light on the relationship between the presence of different ^{13}C NMR functional groups and the applied FSM (Figure 8) as well as the fire behaviour observations recorded during this experiment

(Figure 9). In the first PCA biplot (Figure 8) we see that most of the PyC produced by flanking fires is associated with the N-alkyl, O-alkyl and di-O-alkyl functional groups. For heading fires, most PyC is associated with the O-aryl and alkyl function groups. For backing fires, PyC is roughly equally split between the O-aryl/alkyl and N-alkyl/O-alkyl/di-O-alkyl functional groups. Finally, the loadings in Figure 8 show that the N-alkyl, O-alkyl and di-O-alkyl functional groups are located on the opposite side of the PCA biplot to the aryl and O-aryl functional groups with these two groups showing a strong degree of anti-correlation.

In the second PCA biplot (Figure 9), the relationship between all burnt fuel samples, their ^{13}C NMR composition as well as their relationship with the fire behaviour variables from Table 1 is shown. There are four main clusters within this graph. In the top right quadrant, we see that one of the temperature residence times (i.e. time above 500 ° C; but not 250 ° C or 750 ° C), maximum temperature and the combustion factor are associated with the relative amount of the aryl carbon functional group. In the top left quadrant, the duration of flaming combustion, the time above 250 ° C and 750 ° C as well as the charring intensity are associated. In the bottom left quadrant, the N-alkyl, O-alkyl and di-O-alkyl functional groups are roughly parallel and are anti-correlated with the aryl and O-aryl functional groups. In the bottom right quadrant, the duration of smouldering combustion, Byram fireline intensity, rate of spread, the $\Delta CO/\Delta CO_2$ emissions ratio and fuel moisture content are all roughly parallel and correlated.

4 Discussion

4.1 Properties of PyC

Statistical testing for the differences in ^{13}C NMR composition showed that aryl carbon present in ash was higher for heading fires compared to flanking fires. All other tests for

statistical significance between different burnt fuel samples (including total PyC production) were insignificant. This may be considered a surprising result since insights from the thermokinetics of biomass combustion suggest that fire behaviour, including the influence of FSM, has the potential to alter the type and amount of PyC that remains on the ground after fire (Sullivan, 2007; Sullivan and Ball, 2012; Ball, 2014). Ball et al. (2004) proposed a model whereby flame dynamics act as a thermochemical oscillator with combustion periodically switching between the production of volatiles and that of char. When applied to a propagating fire, available evidence suggests that the combustion pathways associated with heading fire combustion would be directed towards the production of volatiles (e.g. gas phase combustion products) while preferential formation of char would occur from backing as well as flanking fires. Based on the current experiments, there does not appear to be very strong empirical support for the hypothesis that FSM affects the type of carbon functional groups present in PyC. Having said that, it is worth emphasising that the temperature residence times in our experiment (i.e. charring intensities) did not exhibit wide variations which would have limited the amount of char combustion that actually occurred. This conclusion is supported by results from Santin et al. (2017) who suggest that the charring intensity metric (i.e. a measure of temperature residence time) plays a critical role in PyC production. Inclusion of larger fuel elements could potentially change the results we found since coarse woody debris is quite often not fully consumed during the passage of a fire front, leaving PyC in the form of charcoal after fire (Sullivan et al., 2018).

4.2 Insights on PyC

Figure 6 shows that the flanking FSM presented the smallest changes in overall ^{13}C NMR composition due to fire. For twig samples exposed to flanking fires, there is less overall change in the functional groups containing carbon that were present compared to heading and backing fires. In such cases, twigs have been exposed to flame without significant charring,

which raises the issue of where thermal modification of biomass must sit on the combustion continuum to qualify as PyC. Inconsistencies in definitions related to PyC have been raised previously (Zimmerman and Mitra, 2017), which is partially reflective of the differing disciplinary needs of the biogeochemistry (Santin et al., 2016) and atmospheric science communities (Kuhlbusch, 1998; Bond et al., 2013). In the context of the current study, ^{13}C NMR spectroscopy offered the opportunity to confirm that thermochemical modifications were achieved to burnt fuels. This may be considered a benefit of our approach for defining PyC rather than relying on visual assessment methods that are common within the field (Santin et al., 2015; Santin et al., 2016).

4.3 Implications for carbon management in forests

Given that the composition of PyC exists on a continuum (Zimmerman and Mitra, 2017), different functional groups that make up PyC will exhibit different degrees of resistance to biological decomposition (Hilscher and Knicker, 2011). Functional groups such as aryl and O-aryl carbon, which are typically associated with char formation, are more resistant to decomposition (Hilscher and Knicker, 2011) implying that PyC with increased levels of these two functional groups can potentially be locked into the pedosphere for longer periods of time once incorporated into soils. From a carbon management perspective, this is a favourable outcome since converting burnt biomass to aryl or O-aryl carbon prevents the accumulation of carbon in the atmosphere stemming from the decomposition of more degradable forms of carbon such as alkyl, N-alkyl and O-alkyl carbon (Hilscher and Knicker, 2011). While making this observation, it is important to qualify that the resistance of PyC to biological degradation, in general, hinges heavily on the microbial community present in soils (Zimmerman et al., 2011) which will itself depend on soil properties and climate conditions (Cheng et al., 2008).

Although only one statistically significant result was observed (i.e. for the increase in aryl carbon in ash for heading fires compared to flanking fires) the implications for forest fire carbon management primarily stem from the PCA analysis in Figure 9. In the context of this experiment, the main option for sequestering carbon from these fires is to maximise the total production of aryl and O-aryl carbon. Both of these functional groups have a higher degree of resistance to biological decomposition (Hilscher and Knicker, 2011); hence if aryl and O-aryl carbon were formed during fire and stored in soils this could have positive benefits for the overall carbon balance since PyC could be stored in the soil carbon pool for extended periods of time (Woolf et al., 2010). This outcome would be achieved since recalcitrant carbon would be produced and sequestered at the expense of carbon that could be emitted to the atmosphere or stored in soils involving functional groups that are more labile, or prone to decomposition, (such as N-alkyl, O-alkyl and di-O-alkyl carbon; Hilscher and Knicker (2011)). Based on the current results, it appears there are two main strategies to maximise the production of aryl and O-aryl carbon. This involves 1) maximising the residence time of high temperature combustion and by 2) maximising the combustion factor. Point 2) may seem counterintuitive, but essentially involves a relatively complete burn that produces PyC as opposed to an inefficient burn with high amounts of residual smouldering combustion. Maximising the combustion factor to sequester carbon post-fire concords with the recommendations of the National Wildfire Coordinating Group Fire Use Working Team (2001). Indeed, the idea of applying different FSMs to positively modulate the overall carbon balance ultimately stems from this team. In this report, the National Wildfire Coordinating Group Fire Use Working Team suggest that in homogeneous and non-complex fuel beds that backing fires burn more cleanly and with lower emissions than other spread modes due to consuming fuels with a greater efficiency. Our results (Table 1) confirm the notion that backing fires not only burn more cleanly than heading fires (i.e. in terms of the lower $\Delta CO/\Delta CO_2$ emission ratio), but

383 also with a higher degree of combustion completeness (i.e. in terms of the combustion
384 factor). Maximising the residence time of high temperature combustion also concords with
385 basic insights from the mechanism associated with charcoal production (Antal et al., 1990;
386 Strandberg et al., 2015), which has elevated levels of aryl and O-aryl carbon compared with
387 other types of burnt fuel. Further, it is worth noting that if low intensity FSMs (e.g. backing
388 and flanking fires) did lead to increased storage of PyC this would form the basis of a
389 practical carbon storage system since existing prescribed burning techniques (Chandler et al.,
390 1983; Tolhurst and Cheney, 1999) are partially based around the application of these spread
391 modes that propagate with a reduced Byram fireline intensity (e.g. backing fire ignition,
392 chevron ignition, perimeter ignition) for the purpose of increasing controllability and
393 reducing risks of fire escapes.

394

395 Further evidence from our experiments suggest that carbon storage would be promoted by
396 fires that propagate with an intensity less than that of heading fire. The bottom right quadrant
397 of Figure 9 shows that Byram fireline intensity, rate of spread, duration of smouldering
398 combustion and the $\Delta CO/\Delta CO_2$ all point in roughly the same direction in the PCA biplot and
399 are hence associated. These variables are all associated with heading fires that have a high
400 rate of forward spread and Byram fireline intensity. Further, heading fires are also associated
401 with inefficient smouldering combustion which increases the emissions of CO. Previous
402 results from Surawski et al. (2015) confirm that heading fires emit roughly double the CO
403 emissions of flanking and backing fires. This adds further evidence to the notion that attempts
404 to store carbon from propagating fires would be achieved with FSMs having a lower rate of
405 spread and Byram fireline intensity.

406

5 Conclusions

In this study, we explored the properties of PyC produced by the application of three different FSMs to forest litter fuels burnt in a combustion wind tunnel. ^{13}C NMR spectroscopy was conducted to assess the carbon functional groups present in PyC. Overall, the results from this study are broadly consistent with the findings of Baldock and Smernik (2002) who found that combustion increased the presence of recalcitrant carbon-containing functional groups such as aryl and O-aryl carbon while reducing the concentration of more degradable forms of carbon (such as alkyl and O-alkyl carbon). Only one statistically significant result was found which involved higher aryl carbon levels in ash from heading fires compared to ash from flanking fires. PCA results shed light on the possibility that increasing the residence time of high temperature combustion as well as the combustion factor could be a valid method for increasing the production of aryl and O-aryl carbon from fire provided that incomplete combustion of biomass to PyC can still be achieved. Such actions may have positive benefits for the overall PyC balance through storing recalcitrant carbon in soils for extended periods of time. Although the results from this study are not completely conclusive, there remains the possibility that FSM modulation may allow these carbon sequestration outcomes to be achieved.

As a model ecological system, an experimental fire conducted in a combustion wind tunnel is unlike that encountered in the field with its inherently variable fuel architecture, fuel load, topography and ambient environmental conditions. In our study, we tightly controlled experimental factors such as fuel composition, fuel moisture content, the fuel ignition process and wind speed. While this enabled detailed investigation into the role of different FSMs in shaping ^{13}C NMR composition, there exist a number of possible extensions to this work. This

includes re-designing the fuel architecture of the wind tunnel to include other carbon pools that make a significant contribution to fuel load in dry sclerophyll forests, such as coarse woody debris as well as an understorey. Future investigations exploring ^{13}C NMR composition with different FSMs could also vary some of the variables we held constant such as wind speed, fuel moisture content and fuel load.

Acknowledgements

The authors thank Janine McGowan for her assistance with the NMR experiments and data analysis. The authors also thank Cris Santín and Ron Smernik for reviewing a previous draft. N. C. S thanks Michael Battaglia and Sandra Eady for their support of this project.

References

Andreae, M. O. 2019. Emission of trace gases and aerosols from biomass burning – an updated assessment. *Atmos. Chem. Phys.,* 19**,** 8523-8546.

Antal, M. J., Mok, W. S. L., Varhegyi, G. & Szekely, T. 1990. Review of methods for improving the yield of charcoal from biomass. *Energy & Fuels,* 4**,** 221-225.

Baldock, J. A., Sanderman, J., Macdonald, L. M., Puccini, A., Hawke, B., Szarvas, S. & McGowan, J. 2013. Quantifying the allocation of soil organic carbon to biologically significant fractions. *Soil Research,* 51**,** 561-576.

Baldock, J. A. & Smernik, R. J. 2002. Chemical composition and bioavailability of thermally altered Pinus resinosa (Red pine) wood. *Organic Geochemistry,* 33**,** 1093-1109.

Ball, R. 2014. Regulation of atmospheric carbon dioxide by vegetation fires. *Climate Research,* 59**,** 125-133.

Ball, R., McIntosh, A. C. & Brindley, J. 2004. Feedback processes in cellulose thermal decomposition: implications for fire-retarding strategies and treatments. *Combustion Theory and Modelling,* 8**,** 281-291.

Bird, M. I., Wynn, J. G., Saiz, G., Wurster, C. M. & McBeath, A. 2015. The Pyrogenic Carbon Cycle. *In:* JEANLOZ, R. & FREEMAN, K. H. (eds.) *Annual Review of Earth and Planetary Sciences, Vol 43.*

Bond, T. C., Doherty, S. J., Fahey, D. W., Forster, P. M., Berntsen, T., DeAngelo, B. J., Flanner, M. G., Ghan, S., Kaercher, B., Koch, D., Kinne, S., Kondo, Y., Quinn, P. K., Sarofim, M. C., Schultz, M. G., Schulz, M., Venkataraman, C., Zhang, H., Zhang, S., Bellouin, N., Guttikunda, S. K., Hopke, P. K., Jacobson, M. Z., Kaiser, J. W., Klimont, Z., Lohmann, U., Schwarz, J. P., Shindell, D., Storelvmo, T., Warren, S. G. & Zender, C. S. 2013. Bounding the role of black carbon in the climate system: A scientific assessment. *Journal of Geophysical Research-Atmospheres,* 118**,** 5380-5552.

Bowman, D., Balch, J. K., Artaxo, P., Bond, W. J., Carlson, J. M., Cochrane, M. A., D'Antonio, C. M., DeFries, R. S., Doyle, J. C., Harrison, S. P., Johnston, F. H., Keeley, J. E., Krawchuk, M. A., Kull, C. A., Marston, J. B., Moritz, M. A., Prentice, I. C., Roos, C. I., Scott, A. C., Swetnam, T. W., van der Werf, G. R. & Pyne, S. J. 2009. Fire in the Earth System. *Science,* 324**,** 481-484.

Byram, G. M. 1959. Combustion of forest fuels. *In:* DAVIS, K. (ed.) *Forest Fire Control and Use.* New York: McGraw-Hill.

Carvalho, E. O., Kobziar, L. N. & Putz, F. E. 2011. Fire ignition patterns affect production of charcoal in southern forests. *International Journal of Wildland Fire,* 20**,** 474-477.

Chandler, C., Cheney, P., Thomas, P., Trabuad, L. & Williams, D. 1983. Fire in Forestry 2: Forest Fire Management and Organization. New York.

Chatto, K. & Tolhurst, K. 1997. The development and testing of the Wiltronics T-H fine fuel moisture meter, Research Report No. 46, Fire Managment Branch, Department of Natural Resources and Environment, Melbourne, Victoria.

Cheng, C. H., Lehmann, J., Thies, J. E. & Burton, S. D. 2008. Stability of black carbon in soils across a climatic gradient. *Journal of Geophysical Research-Biogeosciences,* 113**,** 10.

Cruz, M. G., Sullivan, A. L., Gould, J. S., Sims, N. C., Bannister, A. J., Hollis, J. J. & Hurley, R. J. 2012. Anatomy of a catastrophic wildfire: The Black Saturday Kilmore East fire in Victoria, Australia. *Forest Ecology and Management,* 284**,** 269-285.

Forbes, M. S., Raison, R. J. & Skjemstad, J. O. 2006. Formation, transformation and transport of black carbon (charcoal) in terrestrial and aquatic ecosystems. *Science of The Total Environment,* 370**,** 190-206.
Gould, J. S., Sullivan, A. L., Hurley, R. & Koul, V. 2017. Comparison of three methods to quantify the fire spread rate in laboratory experiments. *International Journal of Wildland Fire,* 26**,** 877-883.
Hilscher, A. & Knicker, H. 2011. Carbon and nitrogen degradation on molecular scale of grass-derived pyrogenic organic material during 28 months of incubation in soil. *Soil Biology & Biochemistry,* 43**,** 261-270.
Husson, F., Josse, J., Le, S. & Mazet, J. 2018. FactoMineR: Multivariate Exploratory Data Analysis and Data Mining.
Jenkins, M. E., Bell, T. L., Norris, J. & Adams, M. A. 2014. Pyrogenic carbon: the influence of particle size and chemical composition on soil carbon release. *International Journal of Wildland Fire,* 23**,** 1027-1033.
Jenkins, M. E., Bell, T. L., Poon, L. F., Aponte, C. & Adams, M. A. 2016. Production of pyrogenic carbon during planned fires in forests of East Gippsland, Victoria. *Forest Ecology and Management,* 373**,** 9-16.
Kassambara, A. & Mundt, F. 2017. factoextra: Extract and Visualize the Results of Multivariate Data Analyses.
Keene, W. C., Lobert, R. M., Crutzen, P. J., Maben, J. R., Scharffe, D. H., Landmann, T., Hely, C. & Brain, C. 2006. Emissions of major gaseous and particulate species during experimental burns of southern African biomass. *Journal of Geophysical Research-Atmospheres,* 111.
Krishnaraj, S. J., Baker, T. G., Polglase, P. J., Volkova, L. & Weston, C. J. 2016. Prescribed fire increases pyrogenic carbon in litter and surface soil in lowland Eucalyptus forests of south-eastern Australia. *Forest Ecology and Management,* 366**,** 98-105.
Kuhlbusch, T. A. J. 1998. Black carbon and the carbon cycle. *Science,* 280**,** 1903-1904.
Kuhlbusch, T. A. J., Andreae, M. O., Cachier, H., Goldammer, J. G., Lacaux, J. P., Shea, R. & Crutzen, P. J. 1996. Black carbon formation by savanna fires: Measurements and implications for the global carbon cycle. *Journal of Geophysical Research-Atmospheres,* 101**,** 23651-23665.
Lacaux, J. P., Delmas, R., Jambert, C. & Kuhlbusch, T. A. J. 1996. NOx emissions from African savanna fires. *Journal of Geophysical Research-Atmospheres,* 101**,** 23585-23595.
Le Quere, C., Andrew, R. M., Friedlingstein, P., Sitch, S., Pongratz, J., Manning, A. C., Korsbakken, J. I., Peters, G. P., Canadell, J. G., Jackson, R. B., Boden, T. A., Tans, P. P., Andrews, O. D., Arora, V. K., Bakker, D. C. E., Barbero, L., Becker, M., Betts, R. A., Bopp, L., Chevallier, F., Chini, L. P., Ciais, P., Cosca, C. E., Cross, J., Currie, K., Gasser, T., Harris, I., Hauck, J., Haverd, V., Houghton, R. A., Hunt, C. W., Hurtt, G., Ilyina, T., Jain, A. K., Kato, E., Kautz, M., Keeling, R. F., Goldewijk, K. K., Kortzinger, A., Landschutzer, P., Lefevre, N., Lenton, A., Lienert, S., Lima, I., Lombardozzi, D., Metzl, N., Millero, F., Monteiro, P. M. S., Munro, D. R., Nabel, J., Nakaoka, S., Nojiri, Y., Padin, X. A., Peregon, A., Pfeil, B., Pierrot, D., Poulter, B., Rehder, G., Reimer, J., Rodenbeck, C., Schwinger, J., Seferian, R., Skjelvan, I., Stocker, B. D., Tian, H. Q., Tilbrook, B., Tubiello, F. N., van der Laan-Luijkx, I. T., van der Werf, G. R., van Heuven, S., Viovy, N., Vuichard, N., Walker, A. P., Watson, A. J., Wiltshire, A. J., Zaehle, S. & Zhu, D. 2018. Global Carbon Budget 2017. *Earth System Science Data,* 10**,** 405-448.
Masiello, C. A. 2004. New directions in black carbon organic geochemistry. *Marine Chemistry,* 92**,** 201-213.

McArthur, A. 1967. Fire Behaviour in Eucalypt Forests, Forest and Timber Bureau Leaflet No. 107, Commonwealth of Australia, Canberra.
Mulvaney, J. J., Sullivan, A. L., Cary, G. J. & Bishop, G. R. 2016. Repeatability of free-burning fire experiments using heterogeneous forest fuel beds in a combustion wind tunnel. *International Journal of Wildland Fire,* 25**,** 445-455.
National Wildfire Coordinating Group Fire Use Working Team 2001. Smoke Management Guide for Prescribed and Wildland Fire. *In:* HARDY, C. C., OTTMAR, R. D., PETERSON, J. L., CORE, J. E. & SEAMON, P. (eds.).
Page, S. E., Siegert, F., Rieley, J. O., Boehm, H.-D. V., Jaya, A. & Limin, S. 2002. The amount of carbon released from peat and forest fires in Indonesia during 1997. *Nature,* 420**,** 61-65.
Pena, E. A. & Slate, E. H. 2006. Global Validation of Linear Model Assumptions. *Journal of the American Statistical Association,* 101**,** 341-354.
Pena, E. A. & Slate, E. H. 2019. Global Validation of Linear Models Assumptions. 1.0.0.3 ed.
Penman, T. D., Christie, F. J., Andersen, A. N., Bradstock, R. A., Cary, G. J., Henderson, M. K., Price, O., Tran, C., Wardle, G. M., Williams, R. J. & York, A. 2011. Prescribed burning: how can it work to conserve the things we value? *International Journal of Wildland Fire,* 20**,** 721-733.
Plucinski, M. P., Sullivan, A. L. & Hurley, R. J. 2017. A methodology for comparing the relative effectiveness of suppressant enhancers designed for the direct attack of wildfires. *Fire Safety Journal,* 87**,** 71-79.
Pyle, L. A., Hockaday, W. C., Boutton, T., Zygourakis, K., Kinney, T. J. & Masiello, C. A. 2015. Chemical and Isotopic Thresholds in Charring: Implications for the Interpretation of Charcoal Mass and Isotopic Data. *Environmental Science & Technology,* 49**,** 14057-14064.
Raison, R. J., Khanna, P. K. & Woods, P. V. 1985. Transfer of elements to the atmosphere during low-intensity prescribed fires in 3 Australian subalpine eucalypt forests. *Canadian Journal of Forest Research-Revue Canadienne De Recherche Forestiere,* 15**,** 657-664.
Santin, C., Doerr, S. H., Kane, E. S., Masiello, C. A., Ohlson, M., Maria de la Rosa, J., Preston, C. M. & Dittmar, T. 2016. Towards a global assessment of pyrogenic carbon from vegetation fires. *Global Change Biology,* 22**,** 76-91.
Santin, C., Doerr, S. H., Merino, A., Bucheli, T. D., Bryant, R., Ascough, P., Gao, X. & Masiello, C. A. 2017. Carbon sequestration potential and physicochemical properties differ between wildfire charcoals and slow-pyrolysis biochars. *Scientific Reports,* 7.
Santin, C., Doerr, S. H., Preston, C. M. & Gonzalez-Rodriguez, G. 2015. Pyrogenic organic matter production from wildfires: a missing sink in the global carbon cycle. *Global Change Biology,* 21**,** 1621-1633.
Simpson, A. J., McNally, D. J. & Simpson, M. J. 2011. NMR spectroscopy in environmental research: From molecular interactions to global processes. *Progress in Nuclear Magnetic Resonance Spectroscopy,* 58**,** 97-175.
Strandberg, M., Olofsson, I., Pommer, L., Wiklund-Lindström, S., Åberg, K. & Nordin, A. 2015. Effects of temperature and residence time on continuous torrefaction of spruce wood. *Fuel Processing Technology,* 134**,** 387-398.
Sullivan, A. L. 2007. *Competitive Thermokinetics and Non-linear Bushfire Behaviour.* PhD, Australian National University.
Sullivan, A. L. 2017. Inside the Inferno: Fundamental Processes of Wildland Fire Behaviour. *Current Forestry Reports,* 3**,** 132-149.

586 Sullivan, A. L. & Ball, R. 2012. Thermal decomposition and combustion chemistry of
587 cellulosic biomass. *Atmospheric Environment,* 47**,** 133-141.
588 Sullivan, A. L., Knight, I. K., Hurley, R. J. & Webber, C. 2013. A contractionless, low-
589 turbulence wind tunnel for the study of free-burning fires. *Experimental Thermal and*
590 *Fluid Science,* 44**,** 264-274.
591 Sullivan, A. L. & Matthews, S. 2013. Determining landscape fine fuel moisture content of the
592 Kilmore East 'Black Saturday' wildfire using spatially-extended point-based models.
593 *Environmental Modelling & Software,* 40**,** 98-108.
594 Sullivan, A. L., Surawski, N. C., Crawford, D., Hurley, R. J., Volkova, L., Weston, C. J. &
595 Meyer, C. P. 2018. Effect of woody debris on the rate of spread of surface fires in
596 forest fuels in a combustion wind tunnel. *Forest Ecology and Management,* 424**,** 236-
597 245.
598 Surawski, N. C., Sullivan, A. L., Meyer, C. P., Roxburgh, S. H. & Polglase, P. J. 2015.
599 Greenhouse gas emissions from laboratory-scale fires in wildland fuels depend on fire
600 spread mode and phase of combustion. *Atmospheric Chemistry and Physics,* 15**,** 5259-
601 5273.
602 Surawski, N. C., Sullivan, A. L., Roxburgh, S. H., Meyer, C. P. M. & Polglase, P. J. 2016.
603 Incorrect interpretation of carbon mass balance biases global vegetation fire emission
604 estimates. *Nature Communications,* 7**,** 11536.
605 The R Foundation for Statistical Computing 2017. R version 3.4.0.
606 Tolhurst, K. G. & Cheney, N. P. 1999. Synopsis of the knowledge used in prescribed burning
607 in Victoria. East Melbourne, Victoria: Department of Natural Resources and
608 Environment.
609 van der Werf, G. R., Randerson, J. T., Giglio, L., Collatz, G. J., Mu, M., Kasibhatla, P. S.,
610 Morton, D. C., DeFries, R. S., Jin, Y. & van Leeuwen, T. T. 2010. Global fire
611 emissions and the contribution of deforestation, savanna, forest, agricultural, and peat
612 fires (1997–2009). *Atmos. Chem. Phys.,* 10**,** 11707-11735.
613 van der Werf, G. R., Randerson, J. T., Giglio, L., van Leeuwen, T. T., Chen, Y., Rogers, B.
614 M., Mu, M. Q., van Marle, M. J. E., Morton, D. C., Collatz, G. J., Yokelson, R. J. &
615 Kasibhatla, P. S. 2017. Global fire emissions estimates during 1997-2016. *Earth*
616 *System Science Data,* 9**,** 697-720.
617 Wehrens, R. 2011. *Chemometrics with R. Multivariate Data Analysis in the Natural Sciences*
618 *and Life Sciences,* New York, USA, Springer.
619 Wilson, M. A. 1987. *NMR Techniques and Applications in Geochemistry and Soil Chemistry,*
620 Oxford, UK, Pergamon Press.
621 Woolf, D., Amonette, J. E., Street-Perrott, F. A., Lehmann, J. & Joseph, S. 2010. Sustainable
622 biochar to mitigate global climate change. *Nature Communications,* 1**,** 56.
623 Wooster, M. J., Freeborn, P. H., Archibald, S., Oppenheimer, C., Roberts, G. J., Smith, T. E.
624 L., Govender, N., Burton, M. & Palumbo, I. 2011. Field determination of biomass
625 burning emission ratios and factors via open-path FTIR spectroscopy and fire
626 radiative power assessment: headfire, backfire and residual smouldering combustion
627 in African savannahs. *Atmospheric Chemistry and Physics,* 11**,** 11591-11615.
628 Zimmerman, A. R., Gao, B. & Ahn, M. Y. 2011. Positive and negative carbon mineralization
629 priming effects among a variety of biochar-amended soils. *Soil Biology &*
630 *Biochemistry,* 43**,** 1169-1179.
631 Zimmerman, A. R. & Mitra, S. 2017. Trial by Fire: On the Terminology and Methods Used
632 in Pyrogenic Organic Carbon Research. *Frontiers in Earth Science,* 5.
633 Zuur, A. F., Ieno, E. N. & Smith, G. M. 2007. *Analysing Ecological Data,* New York,
634 Springer

635

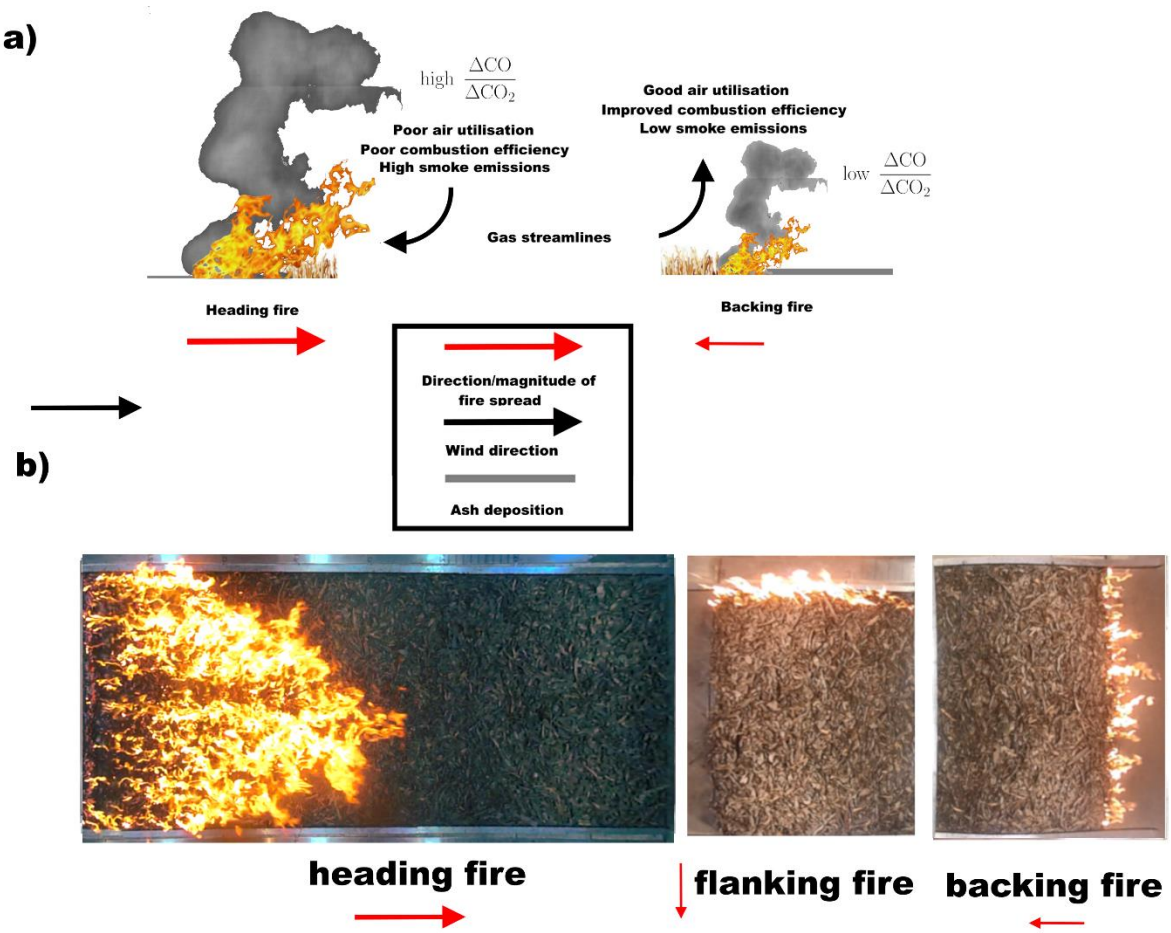

636 **Figure 1:** a) A schematic overview of relevant combustion processes and outcomes
637 for heading and backing fires. In the field, flanking fires (not shown) entail alternating
638 phases of heading or backing fire spread. b) Rectified images of heading, flanking and
639 backing fires in the CSIRO Pyrotron. Wind flow is from left to right for all three
640 FSMs.

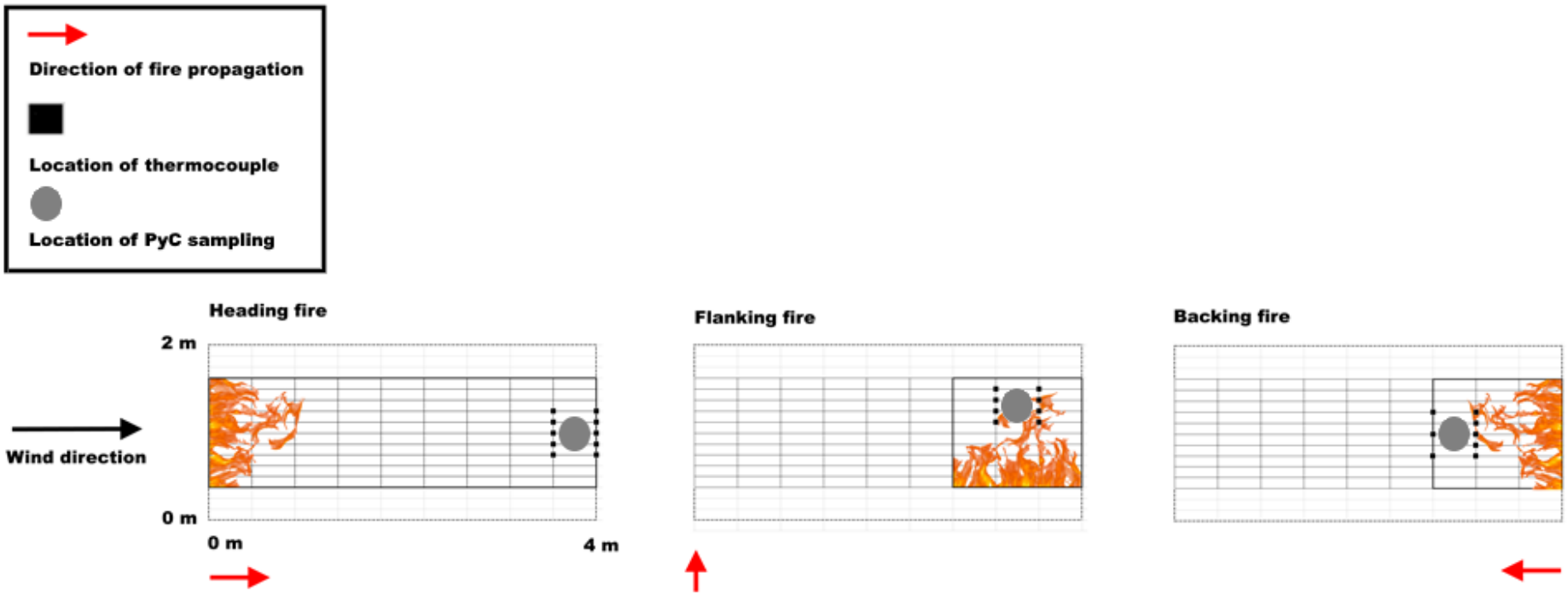

641

642 **Figure 2:** A schematic (not to scale) of the three different FSMs relative to the prevailing wind direction and the location of the K-type

643 thermocouples used for sensing temperatures near the flame base.

Figure 3: An example post-fire fuel bed (from the third backing fire) from which PyC sampling was performed. The left and right hand sides of the fuel bed indicate dimensions (in metres).

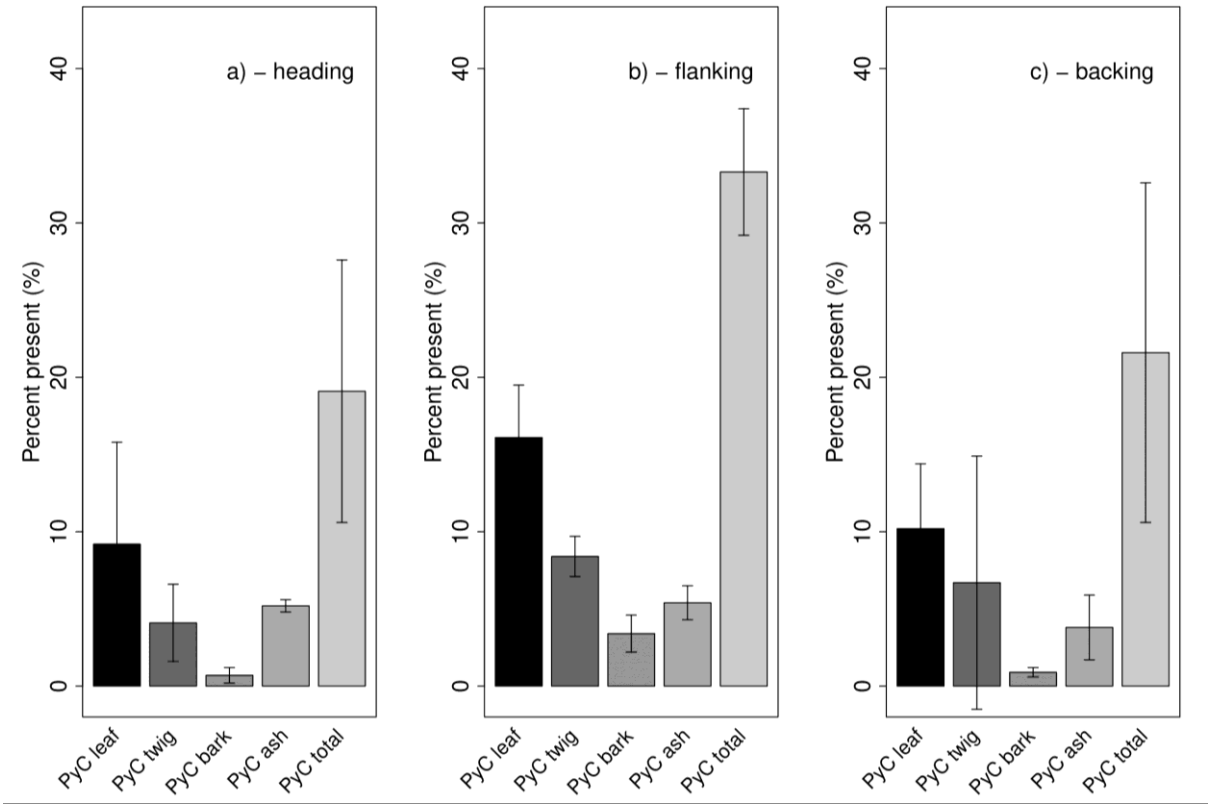

Figure 4: Graphical summary of the contribution of burnt leaves, burnt twigs, burnt bark and ash to total PyC (i.e. total PyC% = PyC burnt leaf% + PyC burnt twig% + PyC burnt bark% + PyC ash%) production for a) heading fires b) flanking fires c) backing fires.

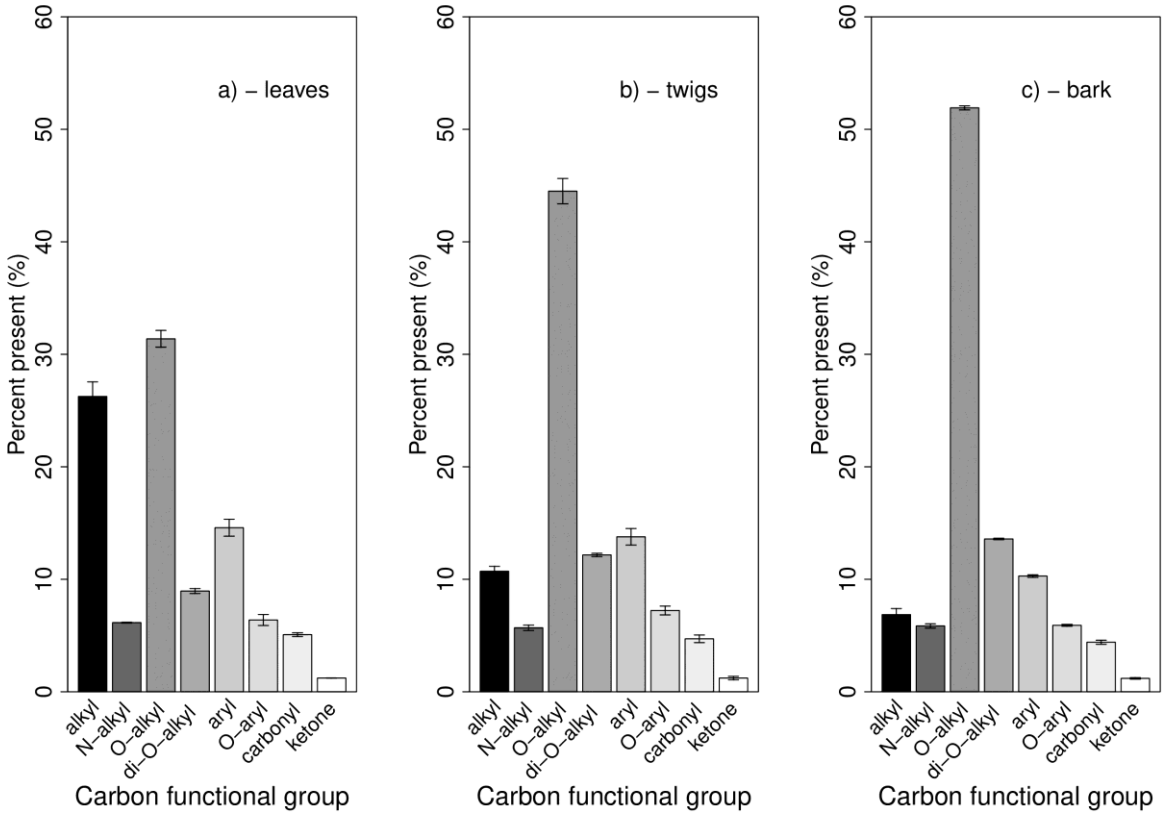

651 **Figure 5:** Graphical summary of the integrated ^{13}C NMR results for different carbon-
652 containing functional groups for unburnt fuels. ^{13}C NMR composition for a) unburnt leaves
653 b) unburnt twigs and c) unburnt bark. Error bars represent the standard deviation based on
654 three replicates.

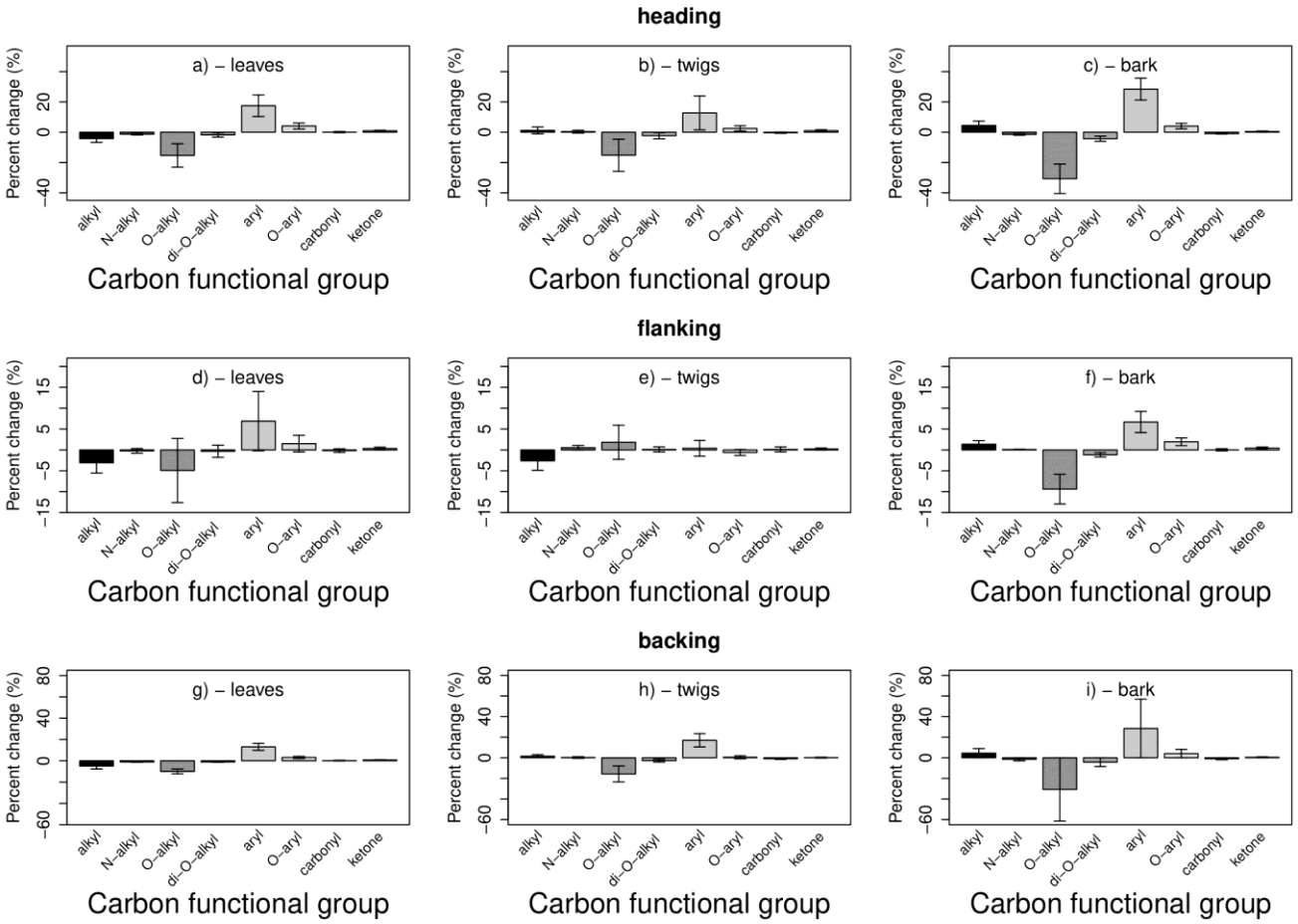

Figure 6: Graphical summary of the integrated ^{13}C NMR results for percentage change in ^{13}C NMR composition for different carbon-containing functional groups for burnt fuels. Percentage change in ^{13}C NMR composition for a) leaves burnt by heading fires b) twigs burnt by heading fires c) bark burnt by heading fires d) leaves burnt by flanking fires e) twigs burnt by flanking fires f) bark burnt by flanking fires g) leaves burnt by backing fires h) twigs burnt by backing fires i) bark burnt by backing fires. Error bars represent the standard deviation based on three replicates.

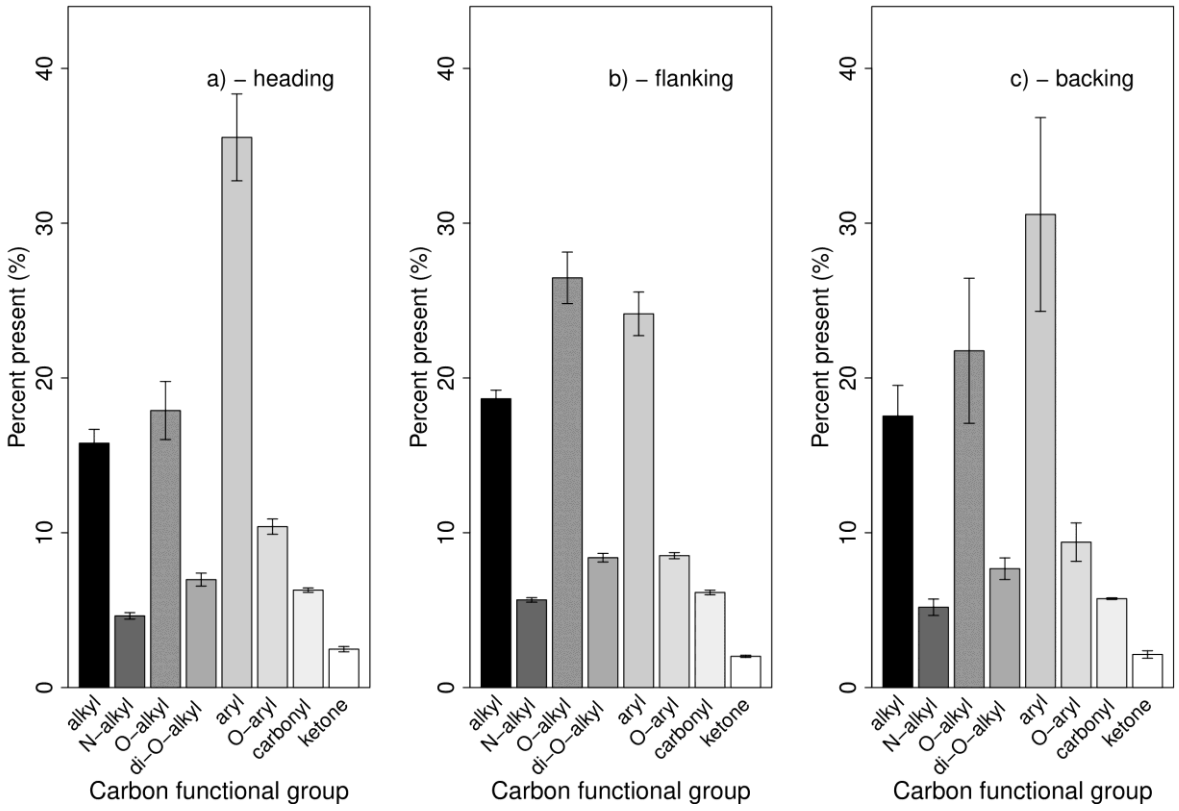

662 **Figure 7:** Graphical summary of the integrated ^{13}C NMR results for different carbon-
663 containing functional groups for ash samples. ^{13}C NMR composition for ash remaining after
664 a) heading fires b) flanking fires and c) backing fires. Error bars represent the standard
665 deviation based on three replicates.

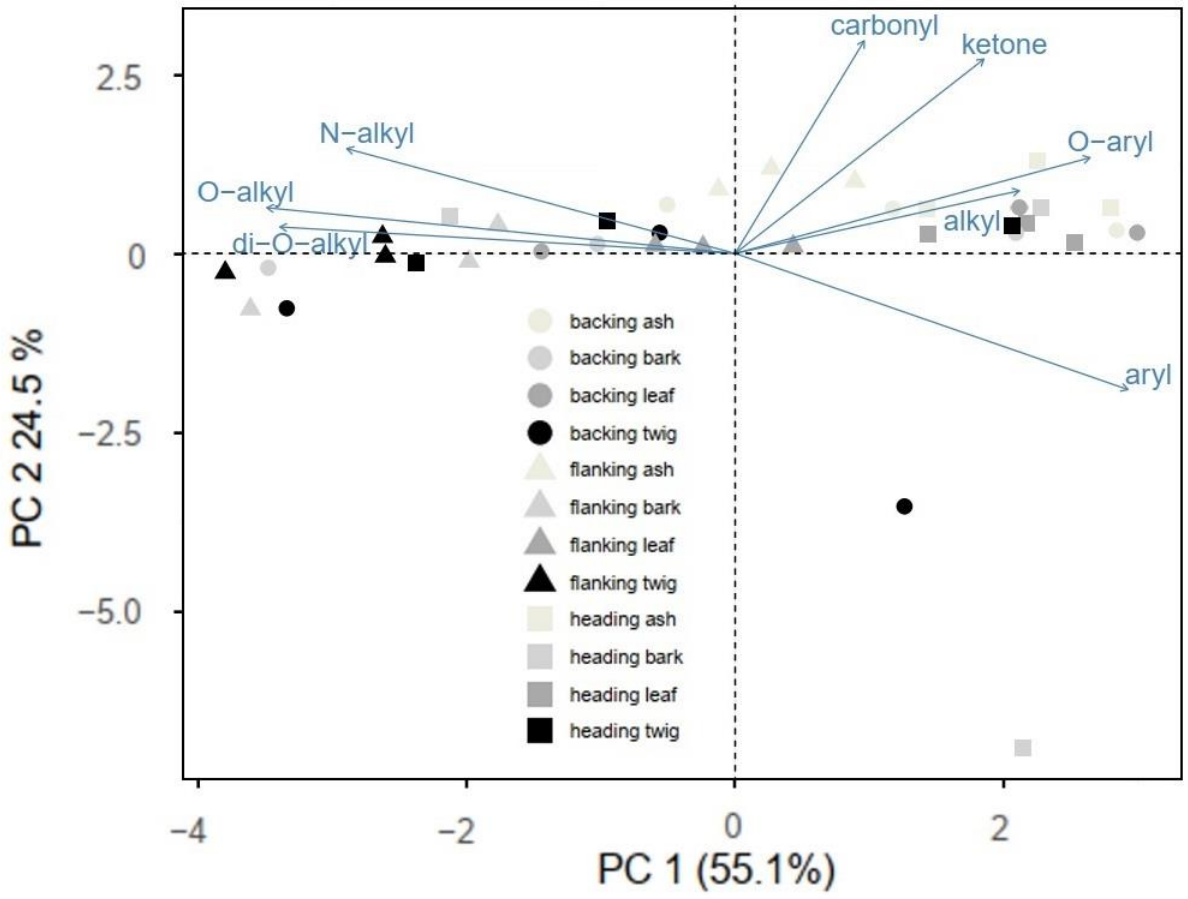

666

667 **Figure 8:** A PCA biplot showing the relationship for different vegetation components
668 burnt with different FSMs and ^{13}C NMR functional groups. The percentage of variance
669 accounted for by each PC is also displayed on each axis.

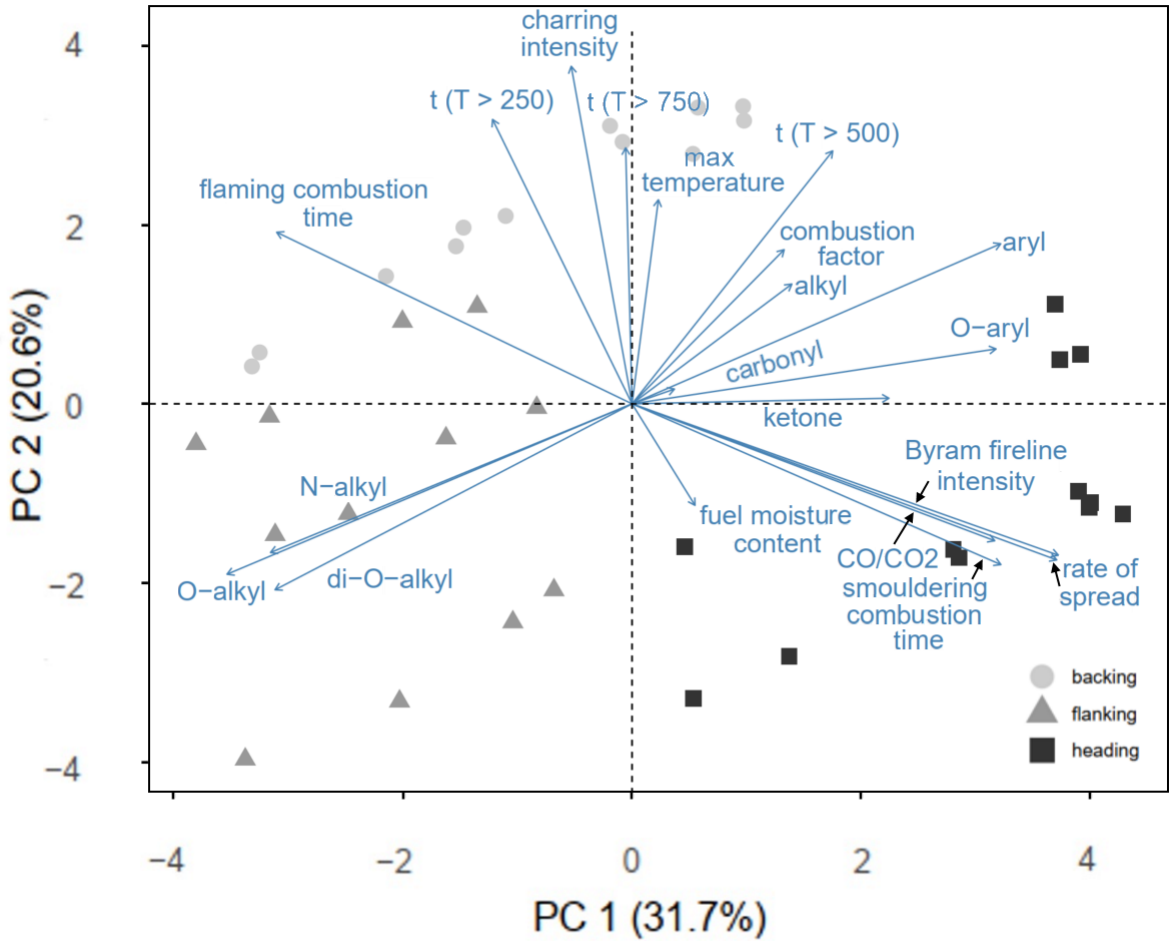

Figure 9: PCA biplot showing the relationship between the fire behaviour variables recorded in this experiment and their ^{13}C NMR composition for different FSMs. The percentage of variance accounted for by each PC is displayed on each axis. Abbreviations used are: t (T > 250), t (T > 500) and t (T > 750) represent the duration of combustion above 250, 500 and 750 °C respectively, max temperature represents the maximum recorded temperature during the fire and CO/CO2 represents the excess mixing ratio for $\Delta CO/\Delta CO_2$.

Table 1: Key fire behaviour variables recorded during this experiment that may affect the properties of PyC. Mean values are provided with the range presented as (minimum value-maximum value). Temperature measurements were made with thermocouples at the locations indicated in Figure 2.

Fire Spread Mode	Fuel moisture content (%)	Flaming combustion duration (s)	Smouldering combustion duration (s)	Rate of spread (m h^{-1})	Combustion factor (%)	Byram fireline intensity (kW m^{-1})*	Charring intensity × 10^4 (°C s) ǂ	Time above 250 °C (s)‖	Time above 500 °C (s)	Time above 750 °C (s)	Maximum temperature °C	ΔCO/ΔCO_2 (-)|
Heading	5.8 (5.1-6.8)	262 (239-290)	514 (390-582)	108 (103-113)	80 (78-83)	472 (462-488)	6.4 (6.1-6.9)	121 (116-128)	58 (54-64)	1.0 (0.5-1.5)	792 (785-801)	0.141 (0.114-0.158)
Flanking	5.6 (5.2-6.2)	907 (769-993)	136 (127-151)	6.7 (5.8-8.2)	73 (70-78)	27 (23-32)	6.5 (4.8-7.7)	130 (99-160)	45 (29-56)	0.3 (0-0.8)	759 (747-768)	0.093 (0.078-0.114)
Backing	5.8 (5.3-6.5)	1407 (1089-1988)	176 (76-242)	5.6 (4.2-6.6)	83 (78-85)	25 (20-31)	7.5 (6.9-7.9)	139 (133-143)	59 (56-64)	3.3 (2.1-4.9)	836 (790-870)	0.098 (0.080-0.107)

* Byram fireline intensity (Byram, 1959) represents the product of the lower heating value of the fuel (kJ kg^{-1}), fuel consumption (kg m^{-2}) and rate of spread (m s^{-1}).

ǂ Charring intensity (CI; Pyle et al., 2015) was obtained by integrating the thermocouple data, T(t), from when the temperature rose to 200 °C (t_0) to when it fell back to 200 °C (t_f) i.e. $\mathrm{CI} = \int_{t_0}^{t_f} T(t)dt$.

‖ Flame arrival at a particular location in the fuel bed occurred when the temperature exceeded 250 °C (Gould et al., 2017).

| ΔX denotes the excess mixing ratio for species X i.e. $\Delta X = X_{plume} - X_{ambient}$.

686 **Table 2:** Assignment of ^{13}C NMR spectral regions to different carbon-containing functional
687 groups. Spectral region assignments are based on Baldock et al. (2013).

Chemical shift limits (ppm)	Proposed dominant type of organic carbon
290-265	Carbonyl and amide spinning side band
265-245	O-aryl spinning side band
245-215	Aryl spinning side band
215-190	Ketone carbon
190-165	Carbonyl and amide carbon
165-145	O-aryl carbon (phenolic and furan)
145-110	Aryl and unsaturated carbon
110-90	Di-O-alkyl carbon
90-65	O-alkyl carbon
65-45	Methoxyl and N-alkyl carbon
45-0	Alkyl carbon

688